

M. Akbari¹

e-mail: dr.mohsen.akbari@gmail.com

A. Tamayol

Biomedical Engineering Department,
McGill University,
Montreal, QC, H3A 1A4, Canada;
Center for Biomedical Engineering,
Department of Medicine,
Brigham and Women's Hospital,
Harvard Medical School,
Cambridge, MA 02139;
Harvard-MIT Division of Health
Sciences and Technology,
Massachusetts Institute of Technology,
Cambridge, MA 02139

M. Bahrami

Laboratory for Alternative Energy
Conversion (LAEC),
Mechatronic System Engineering
School of Engineering Science,
Simon Fraser University,
Surrey, BC, V3T 0A3, Canada

A General Model for Predicting Low Reynolds Number Flow Pressure Drop in Non-Uniform Microchannels of Non-Circular Cross Section in Continuum and Slip-Flow Regimes

A general model that predicts single-phase creeping flow pressure drop in microchannels of a noncircular cross section under slip and no-slip regimes is proposed. The model accounts for gradual variations in the cross section and relates the pressure drop to geometrical parameters of the cross section, i.e., area, perimeter, and polar moment of inertia. The accuracy of the proposed model is assessed by comparing the results against experimental and numerical data collected from various studies in the literature for a wide variety of cross-sectional shapes. The suggested model can be used for the design and optimization of microsystems that contain networks of microchannels with noncircular cross sections resulting from different fabrication techniques.

[DOI: 10.1115/1.4023785]

1 Introduction

The concept of flow through microchannels of arbitrary cross sections forms the basis of a class of applications in microfluidics, which has applications in micromixer designs [1], miniaturized bio/chemical systems [2], flow through porous media [3], cell biology [4], preconcentration and separation of molecules [5,6], and tissue engineering [7,8]. Various techniques are currently in use for liquid handling in microfluidic systems, such as the use of pumps, centrifugal force, electro osmotic flow, and capillary flow. With the exception of electro osmotic flow, in all cases a shear stress induced pressure drop occurs within the channels that needs to be calculated for a successful design.

As a result of recent advances in microfabrication techniques, microchannels with noncircular cross sections are fabricated for both commercial and scientific purposes. For instance, microchannels produced directly by chemical etching on silicon wafers have a trapezoidal cross section [9], while the use of soft lithography [10] or CO₂ laser ablation methods lead to nearly rectangular or triangular cross section microchannels, respectively [11,12]. As a result of this trend, a large number of studies have been focused on flow and pressure drop investigations in straight and variable cross section microchannels with a range of cross-sectional geometries [11,13–17].

Finding analytical solutions for the velocity distribution and, consequently, the pressure drop in complex noncircular cross sections is either case dependent or unlikely; details of the velocity distribution only for few noncircular cross sections have been reported elsewhere [18]. In many applications such as autonomous microfluidic systems [2], serial diluters [19], and microfluidic gradient generators [4], however, the principal of design and

operation is based on the pressure drop rather than the velocity distribution; thus, obtaining a reasonable estimate of the pressure drop of liquid or gas flow in straight or variable cross section microchannels is essential.

In the pertinent literature, there are only a few studies and models focused on the pressure drop in microchannels of general cross sections; see, for example Refs. [17,20–23]. Muzuchka and Yovanovich [20,21] used scale analysis and asymptotic analysis to develop a simple model for predicting the friction factor Reynolds number product of fully developed flow in straight channels of noncircular cross sections. Bahrami et al. [22] developed an approximate model to predict the pressure drop of liquid flow in straight microchannels of arbitrary cross sections. Using the analytical solution of the elliptical duct and the concept of Saint-Venant's principle in torsion, they showed that the Poiseuille number $f Re$ was a function of the polar moment of the inertia, area, and the perimeter of the cross section of the channel. Their model had good agreement with the experimental and numerical data for a wide variety of cross sections such as rectangular, trapezoidal, triangular, circular, and moon-shaped. All aforementioned models, however, were restricted to the no-slip velocity regime and constant cross section channels.

In another study, Bahrami and co-workers [23] extended their model to the slip-flow regime by considering an averaged first-order Maxwell slip boundary condition. They successfully validated their model against existing numerical and experimental data collected from various sources in the literature for several shapes, including circular, rectangular, trapezoidal, and double-trapezoidal cross sections and a variety of gases such as nitrogen, argon, and helium. Tamayol and Bahrami [18] and, later, Tamayol and Hooman [24] developed exact solutions for the flow-field in straight microchannels of noncircular cross section with both continuum and noncontinuum flow regimes, respectively. In another study, Akbari et al. [25] extended the general model of Bahrami et al. [22] to variable cross section microchannels of noncircular shape under the no-slip boundary condition. They showed that the

¹Corresponding author.

Contributed by the Fluids Engineering Division of ASME for publication in the JOURNAL OF FLUIDS ENGINEERING. Manuscript received April 24, 2012; final manuscript received February 14, 2013; published online May 17, 2013. Assoc. Editor: Z. C. Zheng.

pressure drop in slowly-varying cross section microchannels could be obtained from the superposition of a frictional term that was calculated from the lubrication theory and an inertial term, which was a function of the cross-sectional area and flow rate. Their model was successfully validated against experimental data independently obtained in their study or collected from the literature.

In the present study, we will first summarize our previous models for estimation of the pressure drop in straight microchannels of noncircular cross section and then will build on that and develop a unified model that can accurately predict the pressure drop of a low Reynolds number flow in nonuniform microchannels of arbitrary cross section under both slip and no-slip regimes. The proposed unified model postulates that the cross-sectional area varies 'gradually' along the flow direction. The validity of the model is assessed by comparing the results against the available experimental and numerical data from the literature for a wide variety of cross sections.

2 Governing Equations and Theoretical Model

2.1 Straight Channels With No-Slip Velocity Boundary Condition. Consider a fully-developed, steady-state, and laminar flow in a channel with a constant cross-sectional area A_0 and a constant perimeter Γ_0 , as shown in Fig. 1(b). In the absence of the compressibility effects, variation of fluid properties, body forces, and rarefaction and surface effects, the Navier-Stokes equations reduce to the Stokes equation which, in this case, is Poisson's equation [26]

$$\nabla^2 u = \frac{1}{\mu} \frac{dp}{dx} \quad \text{with } u = 0 \quad \text{on } \Gamma \quad (1)$$

where u is the fluid velocity, μ is the dynamic viscosity, and p is the pressure. Exact solutions for the pressure and velocity field in microchannels with elliptical and rectangular cross sections have been reported in many fluid mechanics textbooks; see, for example, Ref. [27]. However, finding exact solutions for many practical cross sections, such as trapezoidal or triangular microchannels, is complex and/or impossible. Therefore, an approximate compact model that can accurately estimate the pressure drop of arbitrary cross sections will be of great value.

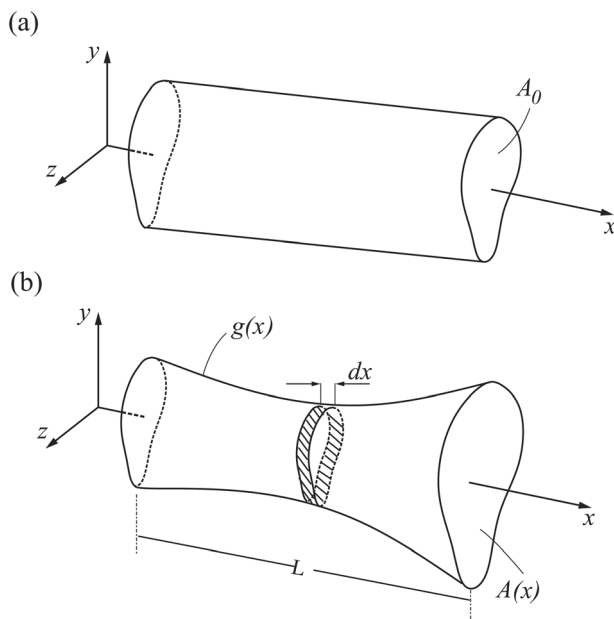


Fig. 1 Schematic of (a) a straight, and (b) a variable cross section microchannel of arbitrary cross section

Here, we propose an approximate model by using the analogy between the laminar fully developed flow in straight microchannels and torsion in beams; the governing equation for both problems is Poisson's equation (Eq. (1)). Comparing various singly connected cross sections, Saint-Venant found that the torsional rigidity of a shaft could be accurately approximated by using an equivalent elliptical cross section, where both the cross-sectional area and the polar moment of inertia are maintained the same as the original shaft. Following a similar approach, one can develop a general and compact model for predicting the pressure drop in straight microchannels of a noncircular cross section [22]

$$f \text{Re}_{\sqrt{A}} = 32\pi^2 I_p^* \frac{\sqrt{A}}{\Gamma} \quad (2)$$

where $I_p^* = I_p/A^2$ is a nondimensional geometrical parameter, I_p is the polar moment of inertia, A is the cross-sectional area, and Γ is the cross-sectional perimeter. The required geometrical parameters used in Eq. (2) are listed in Table 1 for several common cross sections. Note that the characteristic length scale in the definition of the Reynolds number is the square root of the cross-sectional area \sqrt{A} . Using this length scale has been shown to be an appropriate choice in many heat conduction and convection problems [20,22,28], where noncircular geometries are concerned. Equation (2) can be rearranged such that the flow resistance $R = \Delta p/Q$ can be obtained from the following relationship

$$R = \mu \left(\frac{\Gamma L}{2A^2 \sqrt{A}} \right) f \text{Re}_{\sqrt{A}} \quad (3)$$

where L is the channel length and Q is the volumetric flow rate.

2.2 Straight Channels With Slip Condition. It has been shown in the literature that if the molecular mean free path (λ) becomes comparable with the geometrical length scales, then deviations from the continuum models become significant [29]. Therefore, the ratio between λ and the length scale, which is called the Knudsen number, is used as a measure of the deviation from the continuum regime. Based on the Knudsen number, four flow regimes can be considered: continuum (no-slip), slip-flow, transition, and molecular flows [30]. For the slip-flow regime where $0.001 < \text{Kn} < 0.1$, errors due to the use of Navier-Stokes (NS) equations for modeling the bulk flow are negligible [29]. However, deviations in the regions within the vicinity of the solid surfaces become significant; thus, the no-slip boundary condition is no longer valid on walls and a slip-velocity should be considered [31]. It has been shown that for cases where the thermal creep effects on the solid-fluid interface are negligible, the first-order Maxwell boundary condition can be used for the calculation of slip-velocity on the microchannel walls [23,24]

$$u_s = \frac{2 - \sigma}{\sigma} \lambda \frac{\tau_w}{\mu}, \quad \tau_w = \mu \left. \frac{\partial u}{\partial n} \right|_{\text{wall}} \quad (4)$$

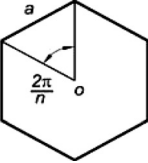
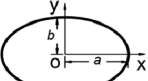
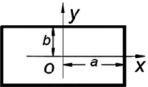
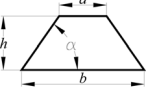
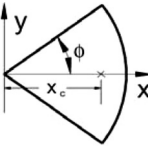
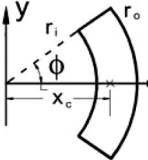
where u_s is the local slip-velocity, τ_w is the local wall shear stress, and σ is the tangential momentum accommodation factor, which is considered equal to one for most engineering applications [32].

Similar to the no-slip regime, finding the analytical velocity solution(s) for complex noncircular cross sections is highly unlikely. Therefore, approximate solutions can be obtained by considering the square root of the cross-sectional area \sqrt{A} as the characteristic length scale and averaging the wall shear stress over the perimeter of the channel. Hence, Eq. (4) becomes

$$\bar{u}_s = \frac{2 - \sigma}{\sigma} \text{Kn} \sqrt{A} \frac{\bar{\tau}_w}{\mu} \quad (5)$$

where \bar{u}_s and $\bar{\tau}_w$ are the average slip-velocity and wall shear stress, respectively. Using an average (and thus constant) slip-velocity

Table 1 Geometrical characteristics of different cross sections

Cross section	Area (A)	Perimeter (Γ)	Non-dimensional polar moment of inertia (I_p^*)
	$\frac{na^2}{4 \tan(\pi/n)}$	na	$\frac{\tan(\pi/n)}{6n} \left(1 + \frac{3}{\tan^2(\pi/n)} \right)$
	$\pi \varepsilon a^{2a}$	$4aE(\sqrt{1-\varepsilon^2})^b$	$\frac{1+\varepsilon^2}{4\pi\varepsilon}$
	εa^{2a}	$4a(1+\varepsilon)$	$\frac{(1+\varepsilon^2)}{12\varepsilon}$
	εh^{2a}	$2h(\varepsilon + \sqrt{\varepsilon^2 - \beta\varepsilon^2 + 1})^c$	$\frac{[(3\varepsilon^2 + 1) + \beta(-3\varepsilon^2 + 1)]\varepsilon}{36}$
	ϕa^2	$2a(1 + \phi)$	$\frac{9\phi^2 - 8 \sin^2 \phi}{18\phi^3}$
	$\phi r_0^2(1 - r^{*2})^d$	$2r_0[(1 - r^*)\phi + 1 - r^*]$	$\frac{\frac{1}{2}(1 - r^{*4}) - \frac{4}{9} \left(\frac{\sin \phi}{\phi} \right)^2 (1 - r^{*3})^2}{\phi(1 - r^{*2})^2}$

^aThe aspect ratio is defined as $\varepsilon = b/a$ for the rectangle and ellipse and $\varepsilon = (a + b)/2h$ for the trapezoid.

^b $E(\varepsilon) = \int_0^{\pi/2} \sqrt{1 - \varepsilon^2 \sin^2 x} dx$ is the complete elliptical function.

^c $\beta = 4ab/(a + b)^2$.

^d $r^* = r_i/r_o$.

one can introduce a relative velocity $U = u - \bar{u}_s$ with a boundary condition of $U = 0$ on the walls; this will significantly simplify the problem. Following the same steps discussed in Ref. [22], a compact relationship for determining the Poiseuille number $fRe_{\sqrt{A}}$ can be obtained as follows

$$fRe_{\sqrt{A}} = \frac{1}{\frac{1}{fRe_{\sqrt{A}}^{no-slip}} + \frac{2-\sigma}{2\sigma} Kn} \quad (6)$$

where $fRe_{\sqrt{A}}^{no-slip}$ is the Poiseuille number for the no-slip condition and can be obtained from Eq. (2).

2.3 Slowly Varying Cross Sections With No-Slip Condition. A schematic of a typical channel with a slowly-varying cross section is illustrated in Fig. 1(b). Finding an analytical solution for such a problem, even for simple geometries such as circular or elliptical cross sections, is highly unlikely. However, approximate solutions have been developed in several studies for circular [33–35] and elliptical [36] cross sections under the assumption of the gradual variation of the cross-sectional area along the flow direction.

Wild et al. [36] showed that for a variable cross section microchannel of elliptical shape, under the creeping flow assumption, the local pressure gradient at each axial location can be obtained from the following relationship

$$-\frac{1}{Q} \frac{dp}{dx} = \frac{4\mu[a^2(x) + b^2(x)]}{\pi a^3(x)b^3(x)} \quad (7)$$

where $a(x)$ and $b(x)$ are the channel local half-major and half-minor axes, respectively, Q is the volumetric flow rate, $A(x)$ is the local cross-sectional area; μ is the dynamic viscosity, and ρ is the fluid density.

Following the similar approach introduced in Ref. [22] and using the cross-sectional square root of the area as the characteristic length scale throughout the analysis, the local Poiseuille number of creeping flow in slowly-varying microchannels of arbitrary cross section can be obtained from the following relationship

$$fRe_{\sqrt{A}}(x) = 32\pi^2 I_p^*(x) \frac{\sqrt{A(x)}}{\Gamma(x)} \quad (8)$$

One can calculate the total flow resistance of a slowly-varying microchannel with arbitrary cross section by using Eqs. (3) and (8) and integrating along the flow direction from the following relationship

$$R = 16\pi^2 \mu \int_{x_1}^{x_2} \frac{I_p^*(x)}{A(x)^2} dx \quad (9)$$

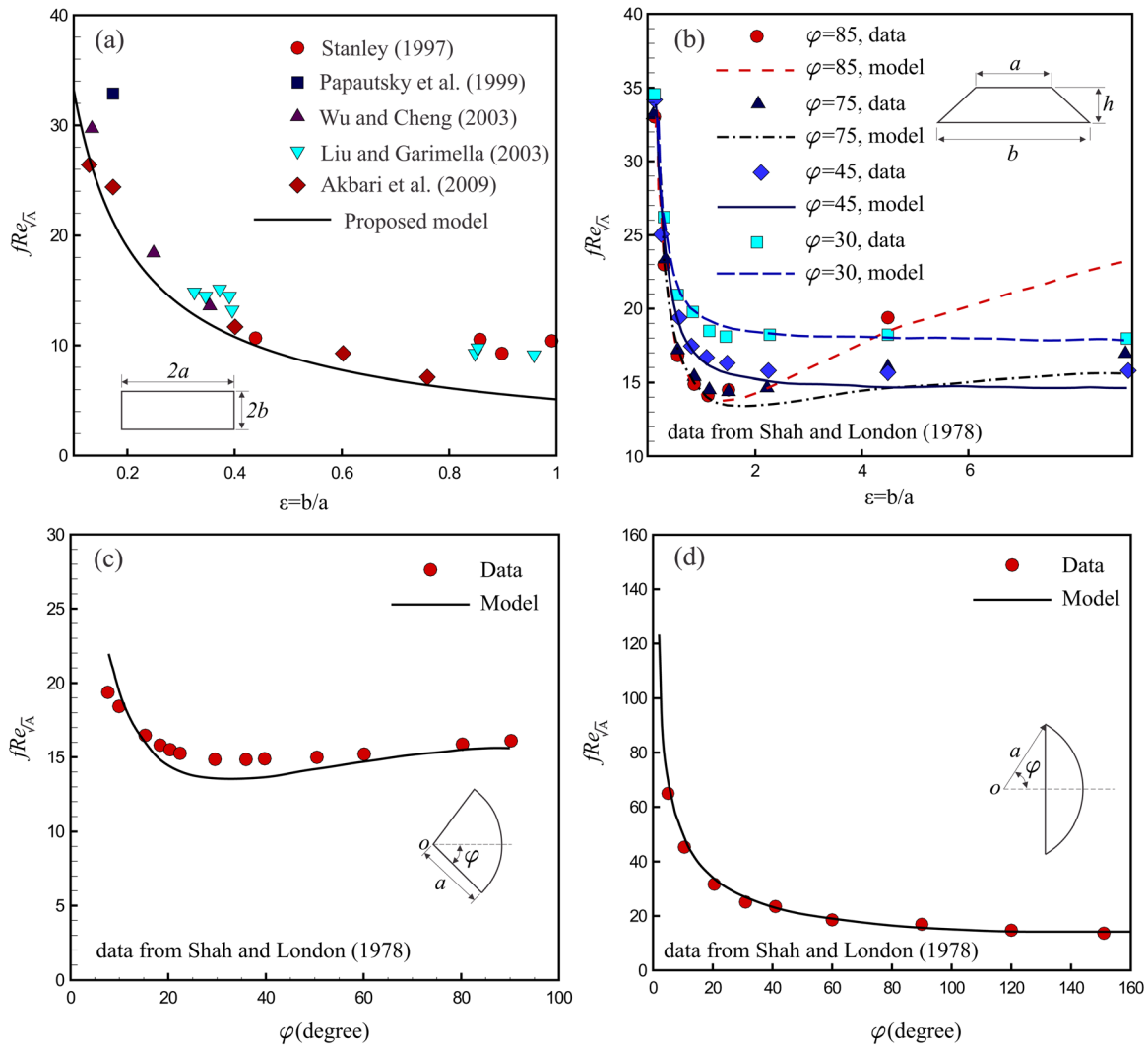


Fig. 2 Comparison of the proposed model for the no-slip condition and the available data for the (a) rectangular [15,38–40], (b) trapezoidal [26], and (c) circular sector [26], and circular segment [26] microchannels

Using Eq. (9) one should note that:

- Equation (9) is a general model, which gives acceptable accuracy when the cross-sectional area gradually varies along the flow direction.
- At the limit where the channel cross section is constant $dA/dx \rightarrow 0$, Eq. (9) predicts the results for straight channels.

2.4 General Model. Following the same steps described in Sec. 2.2, the model presented in Eq. (8) can be extended to cover the slip boundary condition. To this end, it can be concluded that the proposed relationship (Eq. (8)) is a unified model that can be used for calculating the pressure drop in microchannels of slowly varying arbitrary shape cross section subjected to both continuum and slip-flow conditions. In the case of slip-flow through the slowly-varying cross section channels, the local Poiseuille number can be written as

$$fRe_{\sqrt{A}}(x) = \frac{2}{\frac{\Gamma(x)}{16\pi^2\sqrt{A(x)}I_p^*(x)} + \frac{\sigma-2}{\sigma}Kn(x)} \quad (10)$$

The averaged flow resistance of the channel can be written as

$$R = \mu \int_{x_1}^{x_2} \frac{\Gamma(x)}{\left(\frac{\Gamma(x)}{16\pi^2\sqrt{A(x)}I_p^*(x)} + \frac{\sigma-2}{\sigma}Kn(x) \right) A^2(x)\sqrt{A(x)}} dx \quad (11)$$

It is noteworthy that in the case of $Kn \rightarrow 0$, Eq. (11) simplifies to Eq. (9). Thus, Eq. (11) is applicable to continuum and slip-flow through all slowly-varying cross section microchannels and can be considered as the general model. The geometrical parameters that are used in Eq. (11) are summarized in Table 1 for various cross-sectional geometries.

3 Results and Discussion

In this section, the proposed unified model, i.e., Eqs. (10) and (11), is compared against the available experimental and numerical data collected from the literature. It should be noted that for a straight channel, Eq. (8) yields to the model of Bahrami et al. [22], i.e., Eq. (2). In addition, in the case of $Kn \rightarrow 0$, Eq. (10) predicts the fRe values associated with the continuum flow regime. Figure 2(a) shows the comparison of the proposed model

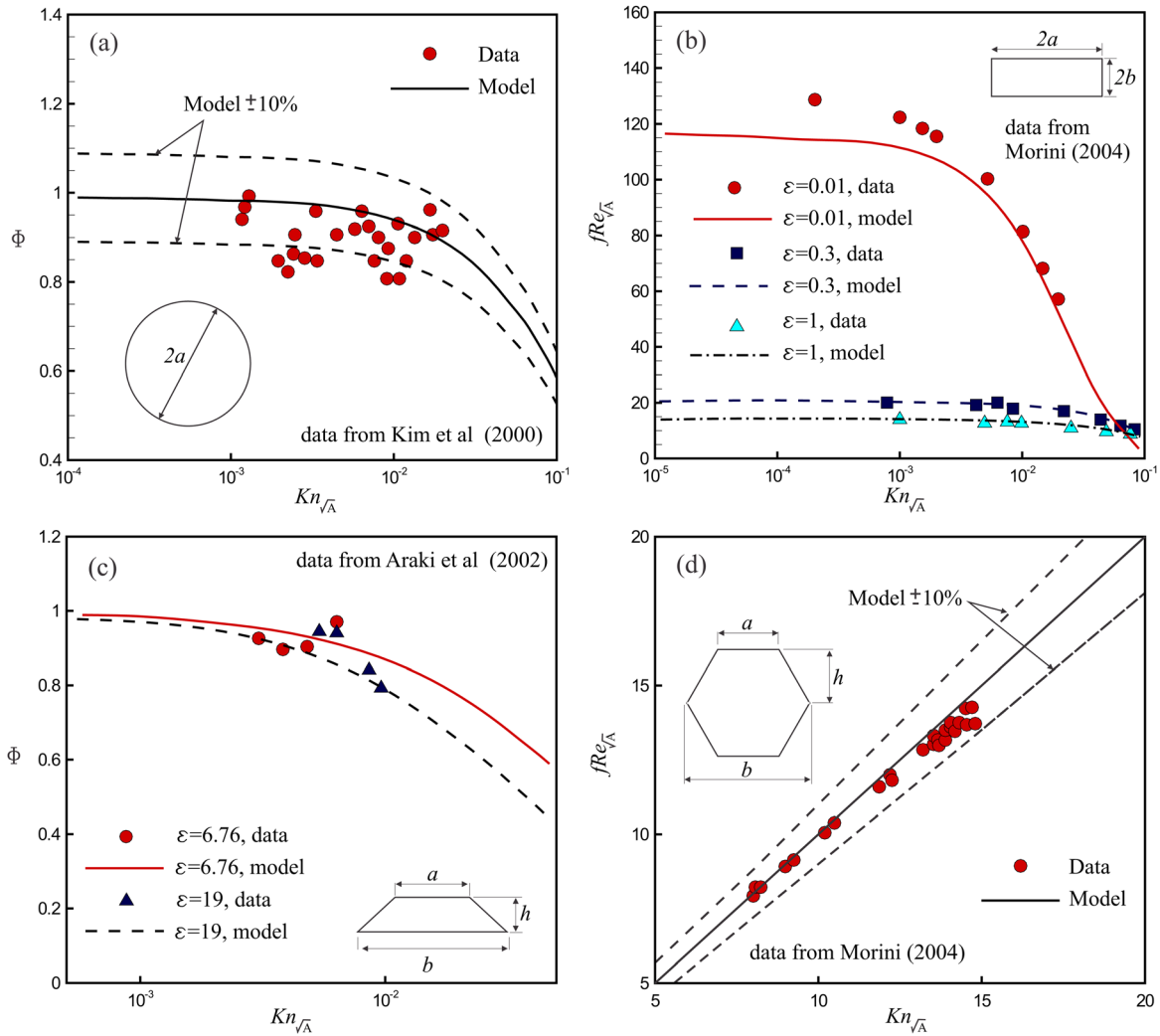


Fig. 3 Comparison of the proposed model for the slip condition and the available data in the literature for the (a) circular (Kim et al. [41]), (b) rectangular (Morini [9]), (c) trapezoidal (Araki et al. [42]), and (d) double-trapezoidal (Morini [9]) cross section microchannels

for the no-slip flow condition against the experimental data of Wu and Cheng [37], Liu and Garimella [15], Stanley [38], Papautsky et al. [39], and Akbari et al. [40] for rectangular cross section microchannels. The collected data covers a wide range of cross-sectional aspect ratios. The solid line represents the analytical model of Eq. (8). As can be seen, the analytical model agrees well with the experimental data over the wide range of the microchannel cross section aspect ratio.

A comparison between the proposed model and the experimental data of Shah and London [26] for trapezoidal cross section microchannels is shown in Fig. 2(b). The $\pm 10\%$ bounds of the model are also shown in the plot, in order to better demonstrate the agreement between the data and the model. In Figs. 2(c) and 2(d), Eq. (8) is compared against the numerical results of Shah and London [26] for the circular sector and circular segment, respectively. It can be seen that the approximate model predicts the trend of the data with acceptable accuracy.

There are few papers in the literature reporting experimental and/or numerical data for the pressure drop of fluid flow in the slip-flow regime. Kim et al. [41] performed an experimental study for three different gases of argon, helium, and nitrogen using quartz-glass microcapillaries with the inner diameter in the range of 5–100 μm . They reported the reduction of the friction coefficient defined as follows against the Knudsen number over a wide range of 0.0008–0.09

$$\Phi = \frac{f\text{Re}_{\sqrt{\lambda}}}{f\text{Re}_{\sqrt{\lambda}}^{\text{no-slip}}} \quad (12)$$

As can be seen in Fig. 3(a), the proposed approach, i.e., Eq. (6), captures the trends of the experimental data over a range of geometrical and thermophysical parameters. In addition, note that most of the data fall within the $\pm 10\%$ bounds of the model.

Figure 3(b) shows the comparison of the proposed model, Eq. (6), with the numerical results of Morini et al. [9] for a rectangular cross section in a range of aspect ratios $0.01 \leq \varepsilon = b/a \leq 1$. As can be seen, except for a few points, the agreement between the model and the numerical values is less than 8%. In Fig. 3(c), the comparison between the proposed model and the experimental data of Araki et al. [42] for trapezoidal microchannels with $\alpha = 54.76$ deg is plotted. They used two different channels with the dimensions: $b = 41.5$ and 41.2 and $h = 5.56$ and $2.09 > \mu\text{m}$, respectively. These channels were fabricated in a silicon wafer with hydraulic diameters of 9.41 and 3.92 μm . They conducted tests with nitrogen and helium over a range of $0.011 < \text{Kn} < 0.035$ and $0.05 < \text{Re} < 4.2$. The uncertainty of their measurements was reported to be 10.9%. As shown in Fig. 3(c), the values predicted by the model are within 10% of the accuracy of the data. Figure 3(d) presents the comparison between the proposed model with the numerical data of Morini et al. [9] for the

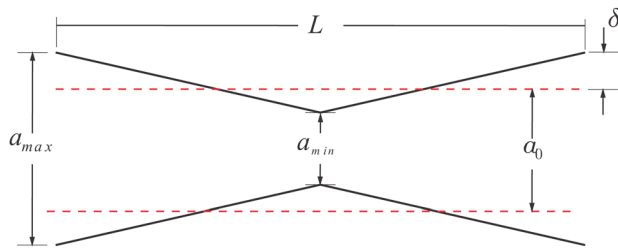


Fig. 4 Schematic of the studied channel with the stream-wise periodic wall with a linear wall profile. The channel cross section is rectangular with constant channel depth.

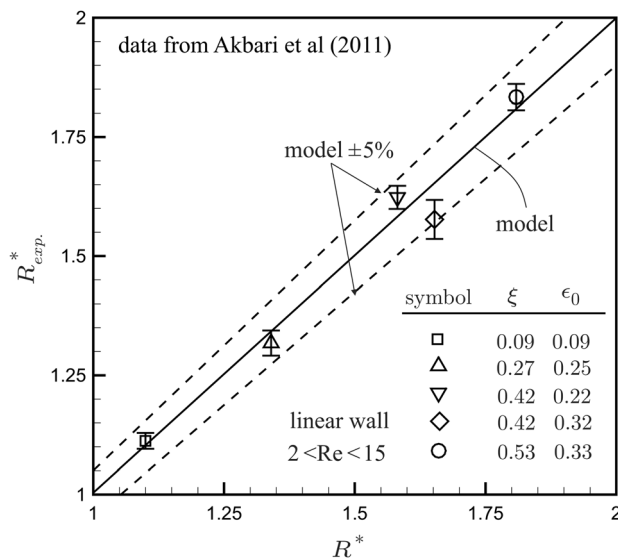


Fig. 5 Comparison of the proposed unified model and experimental data of Akbari et al. [25] for the stream-wise periodic geometry with rectangular cross section. Each data point is averaged over the considered range of Reynolds numbers 2–15. The flow resistance is normalized with a reference straight channel. The geometrical parameters in this plot are the deviation parameter defined as $\xi = \delta/a_0$ and the average aspect ratio defined as $\epsilon_0 = h/a_0$, where h is the channel height, a_0 is the average width of the channel, and δ is the maximum deviation of the channel width from its average.

double-trapezoidal cross section with $\alpha = 54.76$ deg. As can be seen, except for a few points, the agreement between the model and the numerical values is less than 8%.

For stream-wise periodic microchannels of rectangular cross-section, as shown in Fig. 4, we compared the proposed unified model of Eq. (11) with the experimental data obtained by Akbari et al. [25] in Fig. 5. They used the soft lithography method [10] to fabricate microchannels in polydimethylsiloxane with the average hydraulic diameter in the range of 66–140 μm . Pressure drop results were obtained for the Reynolds number range of $2 < \text{Re} < 15$ with distilled water as the working fluid. Since the stream-wise periodic geometry is studied in their work, the Reynolds number effect on the flow resistance has been found to be negligible. Therefore, the average flow resistance over the studied range of Reynolds numbers is reported in Fig. 5. The comparison shows that the experimental data fall within $\pm 5\%$ of Eq. (8).

4 Summary and Conclusions

The pressure drop of low Reynolds number flow in microchannels of arbitrary cross section with gradually varying cross section has been investigated in both the slip and no-slip regimes. A gen-

eral approximate model for the calculation of the pressure drop in noncircular cross section microchannels under the continuum and slip boundary has been developed. The proposed model related the pressure drop to geometrical parameters such as the cross section area, perimeter, and polar moment of inertia. The developed model has been successfully validated against several experimental and numerical data collected from the literature for a wide range of cross-sectional shapes including rectangular, trapezoidal, triangular, double-trapezoidal, circular, circular sector, and annular sector. The proposed model facilitates the preliminary design calculations and optimization of microsystems such as micromixers, microfilters, microreactors, and microchannels filled with porous structures.

Acknowledgment

The authors gratefully acknowledge the financial support of the Natural Sciences and Engineering Research Council of Canada (NSERC). M. Akbari and A. Tamayol acknowledged the NSERC PDF award.

References

- [1] Lauga, E., Stroock, A. D., and Stone, H. A., 2004, "Three-Dimensional Flows in Slowly Varying Planar Geometries," *Phys. Fluids*, **16**, p. 3051.
- [2] Juncker, D., Schmid, H., Drechsler, U., Wolf, H., Wolf, M., Michel, B., de Rooij, N., and Delamarche, E., 2002, "Autonomous Microfluidic Capillary System," *Anal. Chem.*, **74**(24), pp. 6139–6144.
- [3] Gunda, N. S. K., Joseph, J., Tamayol, A., Akbari, M., and Mitra, S. K., 2013, "Measurement of Pressure Drop and Flow Resistance in Microchannels With Integrated Micropillars," *Microfluid. Nanofluid.*, **14**(3-4), pp. 711–721.
- [4] Fatanat-Didar, T., and Tabrizian, M., 2012, "Generating Multiplex Gradients of Biomolecules for Controlling Cellular Adhesion in Parallel Microfluidic Channels," *Lab Chip*, **12**, pp. 4363–4371.
- [5] Kim, S. M., Sommer, G. J., Burns, M. A., and Hasselbrink, E. F., 2006, "Low-Power Concentration and Separation Using Temperature Gradient Focusing via Joule Heating," *Anal. Chem.*, **78**(23), pp. 8028–8035.
- [6] Akbari, M., Bahrami, M., and Sinton, D., 2012, "Optothermal Sample Preconcentration and Manipulation With Temperature Gradient Focusing," *Microfluid. Nanofluid.*, **12**(1), pp. 221–228.
- [7] Khademhosseini, A., Langer, R., Borenstein, J., and Vacanti, J. P., 2006, "Microscale Technologies for Tissue Engineering and Biology," *Proc. Natl. Acad. Sci. U.S.A.*, **103**(8), pp. 2480–2487.
- [8] Tamayol, A., Akbari, M., Annabi, N., Paul, A., Khademhosseini, A., and Juncker, D., 2012, "Fiber-Based Tissue Engineering: Progress, Challenges, and Opportunities," *Biotechnol. Adv.* (in press).
- [9] Morini, G. L., 2004, "Laminar-to-Turbulent Flow Transition in Microchannels," *Nanoscale Microscale Thermophys. Eng.*, **8**(1), pp. 15–30.
- [10] McDonald, J. C., Duffy, D. C., Anderson, J. R., Chiu, D. T., Wu, H., Schueller, O. J. A., and Whitesides, G. M., 2000, "Fabrication of Microfluidic Systems in Poly (Dimethylsiloxane)," *Electrophoresis*, **21**(1), pp. 27–40.
- [11] Oliveira, M. S. N., Alves, M. A., Pinho, F. T., and McKinley, G. H., 2007, "Viscous Flow Through Microfabricated Hyperbolic Contractions," *Exp. Fluids*, **43**(2), pp. 437–451.
- [12] Akbari, M., Sinton, D., and Bahrami, M., 2011, "Geometrical Effects on the Temperature Distribution in a Half-Space Due to a Moving Heat Source," *ASME J. Heat Transfer*, **133**, p. 064502.
- [13] Sparrow, E. M., and Prata, A. T., 1983, "Numerical Solutions for Laminar Flow and Heat Transfer in a Periodically Converging-Diverging Tube, With Experimental Confirmation," *Numer. Heat Transfer, Part A*, **6**(4), pp. 441–461.
- [14] Hemmat, M., and Borhan, A., 1995, "Creeping Flow Through Sinusoidally Constricted Capillaries," *Phys. Fluids*, **7**(9), pp. 2111–2121.
- [15] Liu, D., and Garimella, S. V., 2004, "Investigation of Liquid Flow in Microchannels," *J. Thermophys. Heat Transfer*, **18**(1), pp. 65–72.
- [16] Akbari, M., Sinton, D., and Bahrami, M., 2010, "Laminar Fully Developed Flow in Periodically Converging-Diverging Microtubes," *Heat Transfer Eng.*, **31**(8), pp. 628–634.
- [17] Akbari, M., Sinton, D., and Bahrami, M., 2011, "Viscous Flow in Variable Cross-Section Microchannels of Arbitrary Shapes," *Int. J. Heat Mass Transfer*, **54**(17), pp. 3970–3978.
- [18] Tamayol, A., and Bahrami, M., 2010, "Laminar Flow in Microchannels With Noncircular Cross Section," *ASME J. Fluids Eng.*, **132**(11), p. 111201.
- [19] Kim, C., Lee, K., Kim, J. H., Shin, K. S., Lee, K. J., Kim, T. S., and Kang, J. Y., 2008, "A Serial Dilution Microfluidic Device Using a Ladder Network Generating Logarithmic or Linear Concentrations," *Lab Chip*, **8**(3), pp. 473–479.
- [20] Muzychka, Y., and Yovanovich, M., 2009, "Pressure Drop in Laminar Developing Flow in Noncircular Ducts: A Scaling and Modeling Approach," *ASME J. Fluids Eng.*, **131**(11), p. 111105.
- [21] Muzychka, Y. S., and Yovanovich, M. M., 2002, "Laminar Flow Friction and Heat Transfer in Non-Circular Ducts and Channels—Part I: Hydrodynamic

- Problem," Proceedings of Compact Heat Exchangers: A Festschrift on the 60th Birthday of Ramesh K. Shah, pp. 123–130.
- [22] Bahrami, M., Yovanovich, M. M., and Culham, J. R., 2006, "Pressure Drop of Fully-Developed, Laminar Flow in Microchannels of Arbitrary Cross-Section," *ASME J. Fluids Eng.*, **128**, pp. 1036–1044.
- [23] Bahrami, M., Tamayol, A., and Taheri, P., 2009, "Slip-Flow Pressure Drop in Microchannels of General Cross Section," *ASME J. Fluids Eng.*, **131**, p. 031201.
- [24] Tamayol, A., and Hooman, K., 2011, "Slip-Flow in Microchannels of Non-Circular Cross Sections," *ASME J. Fluids Eng.*, **133**, p. 091202.
- [25] Akbari, M., Bahrami, M., and Sinton, D., 2011, "Viscous Flow in Arbitrary Cross-Section Microchannels of Arbitrary Shape," *Int. J. Heat Mass Transfer*, **54**, pp. 3970–3978.
- [26] Shah, R. K., London, A. L., and White, F. M., 1980, "Laminar Flow Forced Convection in Ducts," *ASME J. Fluids Eng.*, **102**, pp. 256–258.
- [27] White, F. M., 1991, *Viscous Fluid Flow*, McGraw-Hill New York.
- [28] Muzychka, Y. S., and Yovanovich, M. M., 2001, "Thermal Resistance Models for Non-Circular Moving Heat Sources on a Half Space," *ASME J. Heat Transfer*, **123**(4), pp. 624–632.
- [29] Taheri, P., Torrilhon, M., and Struchtrup, H., 2009, "Couette and Poiseuille Microflows: Analytical Solutions for Regularized 13-Moment Equations," *Phys. Fluids*, **21**, p. 017102.
- [30] Roy, S., Raju, R., Chuang, H. F., Cruden, B. A., and Meyyappan, M., 2003, "Modeling Gas Flow Through Microchannels and Nanopores," *J. Appl. Phys.*, **93**, pp. 4870–4879.
- [31] Renksizbulut, M., Niazmand, H., and Tercan, G., 2006, "Slip-Flow and Heat Transfer in Rectangular Microchannels With Constant Wall Temperature," *Int. J. Therm. Sci.*, **45**(9), pp. 870–881.
- [32] Karniadakis, G., Beskok, A., and Aluru, N. R., 2005, *Microflows and Nanoflows: Fundamentals and Simulations*, Springer Verlag, Berlin.
- [33] Manton, M. J., 1971, "Low Reynolds Number Flow in Slowly Varying Axisymmetric Tubes," *J. Fluid Mech.*, **49**(03), pp. 451–459.
- [34] Chow, J. C. F., and Soda, K., 1972, "Laminar Flow in Tubes With Constriction," *Phys. Fluids*, **15**, p. 1700.
- [35] Van Dyke, M., 1987, "Slow Variations in Continuum Mechanics," *Adv. Appl. Mech.*, **25**, pp. 1–45.
- [36] Wild, R., Pedley, T. J., and Riley, D. S., 1977, "Viscous Flow in Collapsible Tubes of Slowly Varying Elliptical Cross-Section," *J. Fluid Mech.*, **81**(02), pp. 273–294.
- [37] Wu, H. Y., and Cheng, P., 2003, "Friction Factors in Smooth Trapezoidal Silicon Microchannels With Different Aspect Ratios," *Int. J. Heat Mass Transfer*, **46**(14), p. 2519.
- [38] Stanley, R. S., Ameel, T. A., and Barron, R. F., 1997, "Two-Phase Flow in Microchannels," DTIC Document.
- [39] Papautsky, I., Ameel, T., and Frazier, A. B., "A Review of Laminar Single-Phase Flow in Microchannels," Proceedings of the International Mechanical Engineers Congress Expos (IMECE), pp. 3067–3075.
- [40] Akbari, M., Sinton, D., and Bahrami, M., 2009, "Pressure Drop in Rectangular Microchannels as Compared With Theory Based on Arbitrary Cross Section," *ASME J. Fluids Eng.*, **131**, p. 041202.
- [41] Kim, M. S., Araki, T., Inaoka, K., and Suzuki, K., 2000, "Gas Flow Characteristics in Microtubes," *JSME Int. J. Ser. B*, **43**(4), pp. 634–639.
- [42] Araki, T., Kim, M. S., Iwai, H., and Suzuki, K., 2002, "An Experimental Investigation of Gaseous Flow Characteristics in Microchannels," *Nanoscale Microscale Thermophys. Eng.*, **6**(2), pp. 117–130.